

# Silent world under COVID-19 – a comprehensive impact analysis based on human mobility

**Shaobin Wang**

Institute of Geographic Sciences and Natural Resources Research, Chinese Academy of Sciences

**Yun Tong**

School of Tourism, Hainan University

**Yupeng Fan**

Institute of Geographic Sciences and Natural Resources Research, Chinese Academy of Sciences

**Haimeng Liu** (✉ [liuhm@igsnr.ac.cn](mailto:liuhm@igsnr.ac.cn))

Institute of Geographic Sciences and Natural Resources Research, Chinese Academy of Sciences

**Jun Wu**

Program in Public Health, Susan and Henry Samueli College of Health Sciences, University of California

**Zheye Wang**

Kinder Institute for Urban Research, Rice University

**Chuanglin Fang**

Institute of Geographic Sciences and Natural Resources Research, Chinese Academy of Sciences

---

## Research Article

**Keywords:** silent index, human mobility, COVID-19, socio-economic activities

**Posted Date:** April 9th, 2021

**DOI:** <https://doi.org/10.21203/rs.3.rs-379845/v1>

**License:**   This work is licensed under a Creative Commons Attribution 4.0 International License.

[Read Full License](#)

---

**Version of Record:** A version of this preprint was published at Scientific Reports on July 19th, 2021. See the published version at <https://doi.org/10.1038/s41598-021-94060-4>.

1 **Silent world under COVID-19 — a comprehensive impact analysis**  
2 **based on human mobility**

3

4 **Shaobin Wang<sup>1</sup>, Yun Tong<sup>2</sup>, Yupeng Fan<sup>1</sup>, Haimeng Liu<sup>1\*</sup>, Jun Wu<sup>3</sup>, Zheyang Wang<sup>4</sup>, Chuanglin**  
5 **Fang<sup>1</sup>**

6 1 Institute of Geographic Sciences and Natural Resources Research, Chinese Academy of Sciences,  
7 Beijing, China

8 2 School of Tourism, Hainan University, Haikou, China

9 3 Program in Public Health, Susan and Henry Samueli College of Health Sciences, University of  
10 California, Irvine, USA

11 4 Kinder Institute for Urban Research, Rice University, Houston, USA

12 \* Corresponding author

13 Email: [liuhm@igsnr.ac.cn](mailto:liuhm@igsnr.ac.cn)

14

## 15 **Abstract**

16 Since spring 2020, the human world seems to be exceptionally silent due to mobility reduction  
17 caused by COVID-19 pandemic. To better measure real-time decline of human mobility and changes  
18 of socio-economic activities in a timely manner, we constructed a silent index (SI) based on  
19 Google's mobility data. We systematically investigated the relations between SI, new COVID-19  
20 cases, government policy, and the level of economic development. Results showed a drastic impact  
21 of the COVID-19 pandemic on increasing SI. The impact of COVID-19 on human mobility varied  
22 significantly by country and places. Bi-directional causality between SI and the new COVID-19  
23 cases was detected, with a lagging period of one to two weeks. The travel restriction and social  
24 policies could immediately affect SI in one week; however, could not effectively sustain in the long  
25 run. Underdeveloped countries are more affected by the COVID-19 pandemic.

## 26 **Introduction**

27 The novel Coronavirus (COVID-19) pandemic is a global threat with escalating health and  
28 social-economic challenges<sup>1,2</sup>. From spring 2020, the human world has been extremely silent during  
29 the COVID-19 pandemic due to several measures practiced globally to slow down the spread of  
30 COVID-19, e.g., social distancing, teleworking, distance learning, banning or reducing crowds,  
31 closing non-essential facilities and services, and staying at home orders. Meanwhile, the Internet  
32 use has increased rapidly to compensate the reduced face-to-face interactions<sup>3</sup>. Although these non-  
33 pharmaceutical interventions effectively reduced the spread of the virus<sup>4,5</sup>, the massive lockdowns  
34 and reduction in human mobility have inadvertently affected global economy for business, transport,  
35 manufacturing, tourism, entertainment, and restaurants<sup>6-9</sup>. It also had great impacts on gender  
36 equality<sup>10</sup>, education<sup>11</sup>, and global poverty<sup>12</sup>. Population-level human mobility data are becoming  
37 increasingly available from location-based services and mobile phone applications<sup>13,14</sup>. During the  
38 COVID-19 crisis, some companies such as Google, Apple, and Facebook publish real-time daily  
39 mobility data to study human movement trends over time<sup>15,16</sup>.

40 Accordingly, the use of mobility data has gained emerging interest in studying the impact of  
41 the COVID-19 pandemic. A large reduction in mobility has been detected globally since the onset  
42 of the COVID-19 threat and administrative restrictions on human interactions<sup>17</sup>. Meanwhile, real-

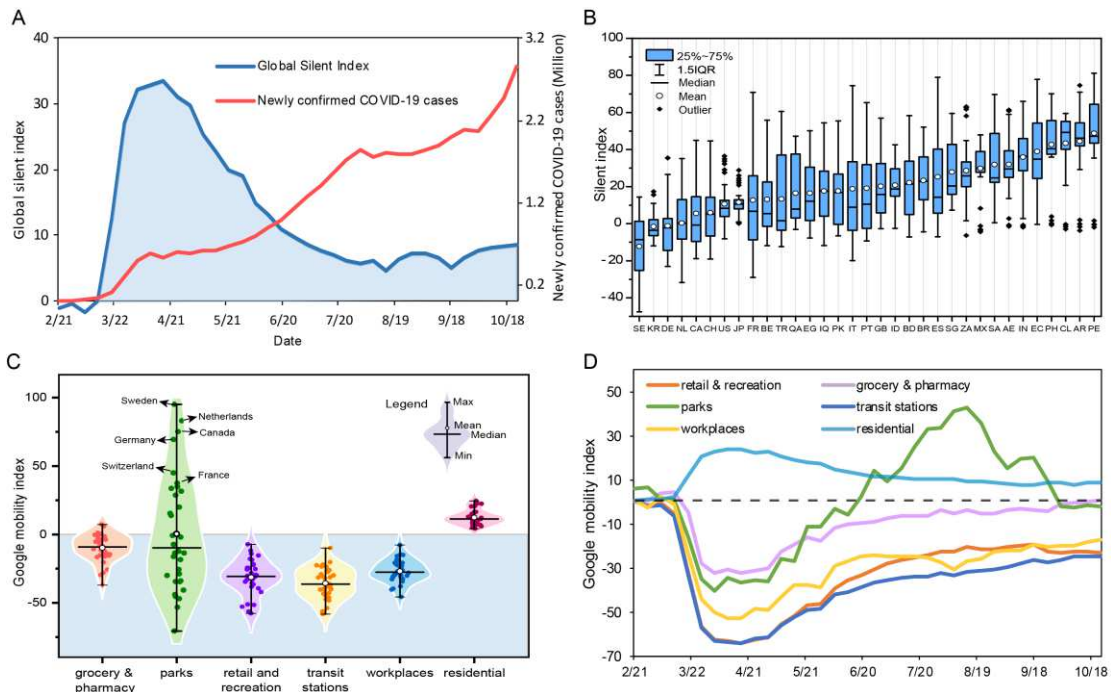
43 time mobility data helped elucidate the COVID-19 transmission and ascertain the implementation  
44 of strict control measures, which substantially mitigated the spread of COVID-19<sup>18-20</sup>. Based on  
45 mobile phone location data, many studies found that reduced population mobility during the  
46 pandemic slowed down the spread of infections<sup>21,22</sup>. Public policies leading to decreased human  
47 mobility was associated with lower COVID-19 cases and deaths<sup>23</sup> and reduced COVID-19 spread<sup>24</sup>.  
48 Similar results were observed across many countries globally<sup>25,26</sup>. However, most data published on  
49 human activity behavior have focused exclusively at a single country, especially in the United States  
50 and Europe<sup>24,27,28</sup>. Meanwhile, few studies have systematically quantified the different relationship  
51 between mobility, COVID-19 cases, and government interventions across countries. Moreover,  
52 some studies have shown that human mobility is strongly associated with regional socio-economic  
53 indicators such as per capita income, poverty rate, unemployment, and education<sup>29-32</sup>. However,  
54 these studies are limited in numbers and focus on the socioeconomic status of a person or family.  
55 There is remarkably little work on evaluating the socio-economic impact of COVID-19 based on  
56 human mobility at country scale.

57 Therefore, in this work, we aim to estimate the global impact of COVID-19 based on human  
58 mobility and to investigate the relations between mobility, new COVID-19 cases, and government  
59 policy across countries over time. The heterogeneity of the relations by place categories and  
60 countries are also discussed. In this study, we constructed a silent index (SI) across countries based  
61 on the Google Community Mobility Dataset, an aggregate of the place-based activity behavior of  
62 millions of individuals in various countries through their location-enabled mobile device data. The  
63 SI was constructed based on five-place categories (retail & recreation, grocery & pharmacy, transit  
64 stations, workplaces, and park), and as a global index by weighting the country-level values by the  
65 total population of each country. The SI was used to comprehensively quantify the daily changes in  
66 human mobility and served as a proxy indicator of change in socio-economic activities (see  
67 Methods). We examined the potential relations between SI, new COVID-19 cases and government  
68 policy using Panel vector autoregression (PVAR) and Impulse response function (IRF). We  
69 demonstrate that a large-scale and holistic picture of the global shock of COVID-19 can be obtained  
70 based on the real-time daily mobility data with fine temporal granularity.

## 71 **Results**

72 **How silent the world was in 2020 globally, nationally and at specific places?**

73 First, we analyzed the global SI from before the start of the global COVID-19 pandemic in  
 74 February 2020 to mid-October 2020. Fig. 1 compares the number of newly confirmed COVID-19  
 75 cases (red curve) and the global SI (see Methods) based on weekly-data from 126 countries since  
 76 February 15th, 2020. The global SI rose rapidly right after the World Health Organization (WHO)  
 77 announced a pandemic phase on March 11<sup>th</sup>, 2020, with a peak value of 33 in mid-April, followed  
 78 by a consistent decline till August 2020. The average global SI is 12.5 during this period. In  
 79 comparison, the number of newly confirmed daily COVID-19 cases increased since March till  
 80 October 2020 (Fig. 1A).



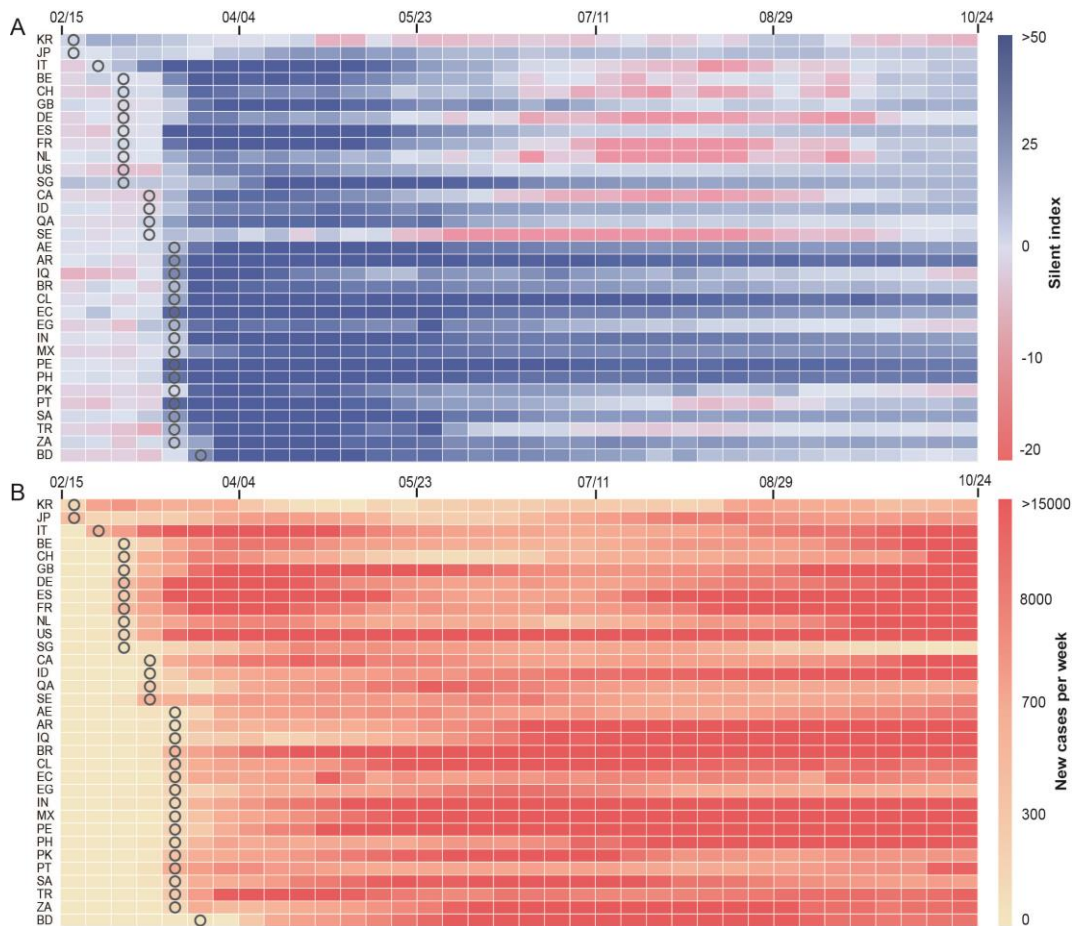
81  
 82 **Figure 1.** Variation of the silent world globally, nationally and by place. (A) Temporal variation of global SI and the number of  
 83 newly confirmed COVID-19 cases from 126 countries from the baseline day to middle October 2020. (B) Box-plot of SI since  
 84 the 100 confirmed COVID-19 cases reported in 33 selected countries. (C) Violin-plot of Google mobility index (see Methods) by  
 85 six place categories in 33 countries. (D) Temporal variation of mobility in six places in 33 countries.

87 Thirty-three countries were selected to closely examine the temporal variation of SI across  
 88 countries. These countries had a high popularity of Google service on mobile phones and  
 89 experienced a relatively serious COVID-19 epidemic. Fig. 1B shows that the SI values varied  
 90 greatly by the country during the pandemic, with the lowest value of -12.29 in Sweden and the  
 91 highest value of 48.75 in Peru. The average SI values were negative in three countries (i.e., Sweden,  
 92 Germany, and South Korea), and positive in other countries, indicating reduced human mobility in

93 these countries compared with that in the baseline period before the pandemic (See Methods for  
94 details of a baseline period). In addition, the range and variation of SI differed greatly among the 33  
95 countries (Fig. 1B). Spain, Ecuador, France, and Italy had the larger range of SI values, while a  
96 number of other countries including the United States, Japan, South Africa, Mexico, Chile, Peru,  
97 Argentina, and the Philippines had some sporadic extreme values (mostly toward the lower end with  
98 some negative values), indicating large fluctuations.

99 The human mobility in specific places showed significant differences in 33 selected countries,  
100 with the largest difference seen for the park and the smallest difference for residences (Fig. 1C). The  
101 average human mobility by place category ranked as: residence > grocery & pharmacy > parks >  
102 workplaces > retail & recreation > transit stations. The residential mobility values in all countries  
103 were positive. As one might expect, people are forced to stay at home, which results in higher  
104 mobility in residential places during the COVID-19 pandemic. Most mobility values in other place  
105 categories were negative except positive values for parks (more park visits) in several countries,  
106 such as Sweden, Netherlands, Canada, Germany, Switzerland, and France.

107 Compared to the pre- COVID-19 period, retail & recreation areas, transit stations, and work  
108 places became the least mobile. Entertainment is the easiest for people to give away. It is also  
109 relatively easy to change to online shopping and tele-commuting or work from home. Grocery and  
110 pharmacy are places that meet people's essential needs thus have less reduced mobility. Parks had  
111 the widest range of Google mobility index values, with some countries having increased park visits  
112 during the pandemic. In addition, the mobility index of grocery & pharmacy, workplaces, retail &  
113 recreation, and transit stations showed a similar trend, with a sharp decline starting in late March  
114 till April followed by gradual increase, but never reaching the pre-epidemic levels at the end of the  
115 study period. The mobility of parks showed a rebound from June to September, 2020, far exceeding  
116 the pre-epidemic level after the reduction in April to May, which may reflect a strong demand for  
117 natural contact after long-term stay-home orders and also more outdoor activities in the warmer  
118 summer time (Fig. 1D).



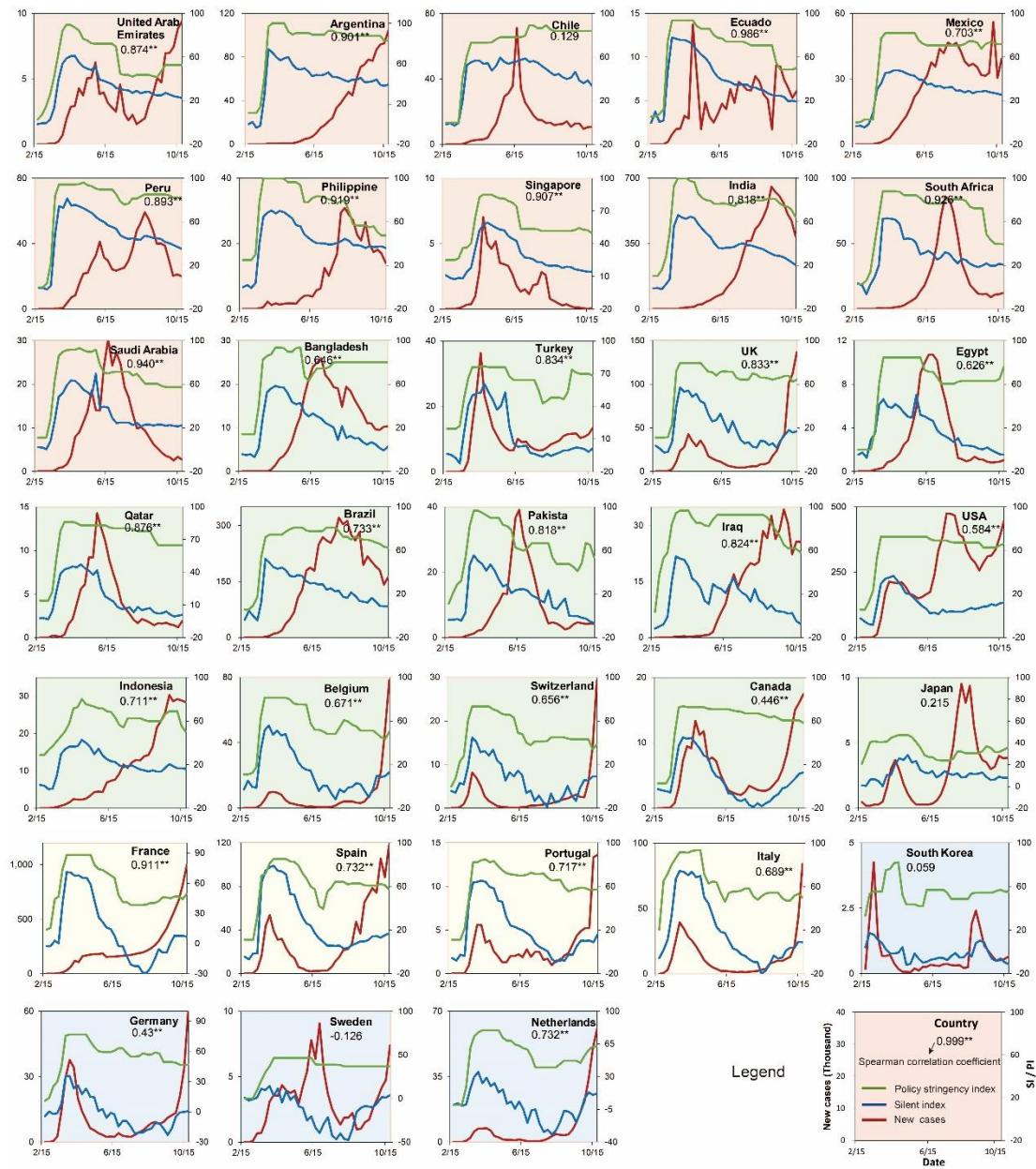
119

120 **Figure 2.** Temporal variations of SI and new COVID-19 cases. The changing of SI (A) and newly confirmed weekly cases of  
 121 COVID-19 (B) in 33 selected countries from the baseline day to late October 2020 were visualized with heatmap. The symbol “o”  
 122 indicated the week when the cumulative number of COVID-19 cases reached 100. The 33 countries’ full names can be seen in  
 123 Table S1.

124 **Temporal variations of SI and new COVID-19 cases**

125 Although most of the 33 countries experienced higher SI during the COVID-19 outbreak  
 126 compared to the period before the outbreak especially from March to May 2020, the magnitude of  
 127 changes in SI varied across countries and over time (Fig. 2A). First, the SI were mostly negative  
 128 before the date when cumulative COVID-19 cases reached 100, indicating that human mobility  
 129 slightly increased compared to that in the baseline period. The SI became positive in most countries,  
 130 especially in Ecuador, Peru, Philippines, Portugal, et al., after the WHO announced the global  
 131 pandemic of COVID-19 on March 11<sup>th</sup>. The result indicates the important role of the WHO  
 132 announcement in providing guidance for individual countries to develop containment and closure  
 133 policies and fast responses that resulted in reduced population movement and contact in the early  
 134 stage of the outbreak. Second, the difference among countries became less pronounced after more  
 135 countries implemented containment and control measures in early March to May 2020. However,

136 the SI decreased sharply in July-September and then rebounded in October in many European  
 137 countries including Belgium, Switzerland, Germany, France, Italy, Netherlands, etc. after  
 138 experiencing high SI values in April and May. This is related to the temporal variations of new  
 139 COVID-19 cases in each country (Fig. 2B). In addition, the SI of South Korea and Sweden stayed  
 140 around 0 and changed little throughout the study period, indicating little impact of the COVID-19  
 141 pandemic on population mobility.



142

143 **Figure 3.** Temporal variation of SI, the new COVID-19 cases, and policy stringency index by countries. Four groups across the  
 144 countries are clustered with different colors by dendrogram in the heatmap of SI (see Fig. S1). Spearman correlations between SI and  
 145 PI are labeled for each country, and \*\* means a significant correlation at the 0.01 level.

146

147 **Relationship between SI, COVID-19 cases, and government policy**

148 Fig. 3 illustrated the temporal variation of SI, the new COVID-19 cases, and the policy  
 149 stringency index (PI, see Methods) by country during the study period. Based on the hierarchical  
 150 clustering of the heatmap of SI variations, we identified four clusters (see Fig. S1). The first cluster  
 151 showed a rapid increase of SI in early March, followed by a gently decline trend afterwards with no  
 152 large fluctuations. The second cluster showed a steep rise of SI in early March and a quick decline  
 153 trend afterwards. The third cluster presented a similarly steep rise as the second cluster, but the peak  
 154 of SI was higher than 60 and declined soon after reaching the peak values; this cluster had the largest  
 155 range of SI values. The fourth cluster had the lowest SI values with small fluctuation.

156 Significant Spearman correlations between SI and PI were identified in 29 out of 33 countries  
 157 (Fig. 3). These 29 countries also experienced an earlier rise in the PI curve than that in the SI curve,  
 158 indicating that the containment and closure policies preceded the decline of human mobility. No  
 159 significant relations between SI and PI were observed in Chile, South Korea, Sweden, and Japan.

160 Furthermore, the panel vector autoregression (PVAR) model was used to examine the dynamic  
 161 relationships between SI, the growth rate of new COVID-19 cases (*D.addcase*), and the policy  
 162 stringency index (PI) using one week as the time granularity. All three variables pass the unit root  
 163 test (see Table S3), indicating that the PVAR models can be constructed. According to the optimal  
 164 lag order test (see Table S4-S5), it can be determined that the optimal lag order of the PVAR models  
 165 was lag 2 stage. The parameters of the PVAR models were estimated using the generalized method  
 166 of moments (GMM) (Table 1). The estimation results all passed the stability condition test (see Fig.  
 167 S2).

168

**Table 1 Results of PVAR analysis**

VARIABLES	(1)	(2)	(3)	(4)
	<i>SI</i>	<i>D.addcase</i>	<i>SI</i>	<i>PI</i>
<i>L.SI</i>	1.2943*** (0.037)	1.1763* (0.678)	1.0792*** (0.060)	0.0371 (0.045)
<i>L2.SI</i>	-0.3424*** (0.037)	-1.2675* (0.703)	-0.0202 (0.047)	0.0299 (0.040)
<i>L.D.addcase</i>	0.0049*** (0.001)	0.3711*** (0.116)		
<i>L2.D.addcase</i>	0.0023** (0.001)	0.2160** (0.089)		

<i>L.PI</i>			0.2389**	1.3306***
			(0.114)	(0.092)
<i>L2.PI</i>			-0.4386***	-0.4705***
			(0.059)	(0.060)
Observations	1,088	1,088	1,122	1,122

169 Standard errors in parentheses, \*\*\* p<0.01, \*\* p<0.05, \* p<0.1

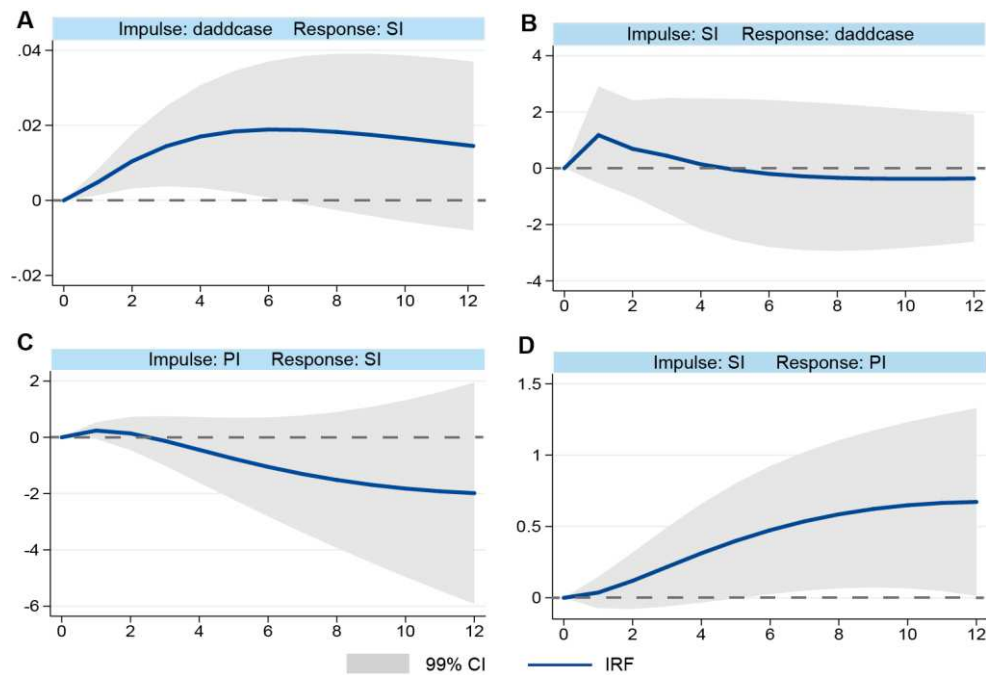
170

171 We found a bidirectional causality relationship between SI and D.addcase. On one hand, the  
172 results showed that the increase of D.addcase with lags one and two weeks significantly promoted  
173 the current SI increase, indicating that the outbreak of the COVID-19 pandemic has had a huge  
174 impact on the mobility, economy, and society of the study countries. On the other hand, the increase  
175 in SI with one-week lagging had a positive impact on D.addcase in this period, but the increase in  
176 SI with two weeks lagging significantly reduced D.addcase in this period, suggesting that the impact  
177 of SI on COVID-19 cases has a time lag, that is, it cannot take effect quickly within a week but may  
178 need at least two weeks to suppress the COVID-19 epidemic.

179 Further, a one-way causality relationship between SI and PI was detected. Specifically,  
180 increased PI with one-week lagging significantly increased SI in the current period, indicating that  
181 the policy implementation can take effect quickly. However, the results of lagging 2 weeks showed  
182 that the implementation of travel restrictions and social policies was difficult to remain effective in  
183 the long run. Meanwhile, PI did not change with the change of SI in the lag period, indicating that  
184 there is a one-way causal relationship between SI and PI.

185 Moreover, a 12-period (week) impulse response function (IRF) was conducted to reveal the  
186 change process of SI responding to D.addcase and PI shocks over a longer period (Fig. 4). First, an  
187 inverted U-shape curve was observed for the impact of D.addcase on SI (Fig. 4A); SI increased  
188 rapidly in 4 weeks, but then flattened and gradually decreased over time. Second, we observed a  
189 lagging response in D.addcase from the impact of SI (Fig. 4B); D.addcase maintained an upward  
190 trend first for about a week, and then decreased over time. Third, we observed a slight rising trend  
191 of SI due to the impact of PI in about a week, followed by a decline trend afterwards (Fig. 4C),  
192 which is consistent with the PVAR results. Last, we observed a positive association between SI and  
193 PI with little lagging response (Fig. 4D), which is likely because both reflect the response of public  
194 and government to the aggravation of the COVID-19 pandemic, as our PVAR analysis showed no

195 direct significant influence of SI on PI.



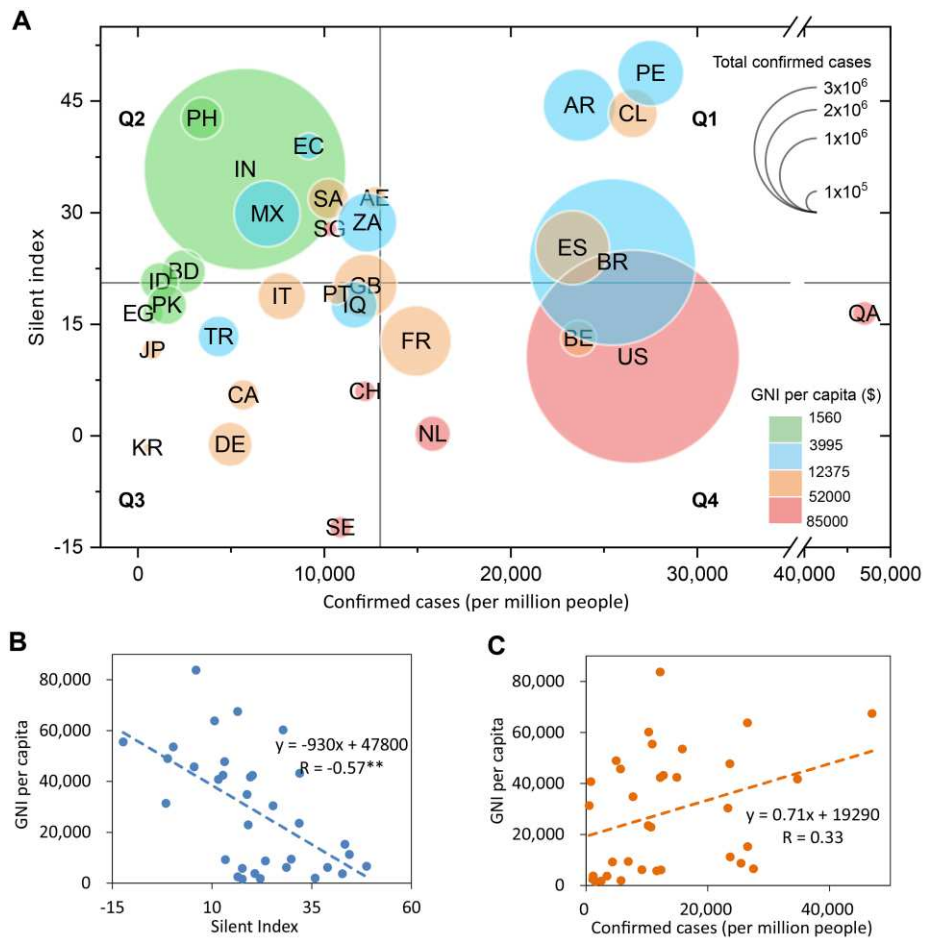
196

197 **Figure 4.** Results of impulse response function (IRF) analysis. Impulse response results were obtained by running  
198 500 iterations of the Monte Carlo Simulation; the upper and lower curves represent the 99% CI. The horizontal axis  
199 indicates the step numbers of the twelve-period impulse response function.

200

### 201 **Does lower income means more silence and larger impacts?**

202 Further analysis of the relationship between SI and confirmed COVID-19 cases per million  
203 population by Oct. 24, 2020 showed that gross national income (GNI) may play a role (Fig. 5A). In  
204 general, SI and GNI per capita have a significant negative linear relationship (Fig. 5B), but GNI per  
205 capita and COVID-19 infection rate showed a weak and insignificant positive relationship (Fig. 5C).  
206 In the quadrantal diagram of SI and standardized COVID-19 cases, most developed countries  
207 (including the United States, Switzerland, Sweden, Singapore, Netherlands, and Qatar) were in the  
208 Q4 region—high incidence rate and low SI. While less developed countries were mostly in the  
209 Q2 region—low incidence rate and high SI (including India, Pakistan, South Africa, Peru,  
210 Ecuador, Mexico, Turkey, and Brazil. Belarus is an exception). For the middle-income countries  
211 (blue circles), SI was positively correlated with the standardized total COVID-19 cases per million  
212 population. During the study period, the economically underdeveloped countries had higher SI,  
213 which likely helped these countries to delay the epidemic spread, but also meant their socio-  
214 economic system were more affected by the COVID-19 pandemic.

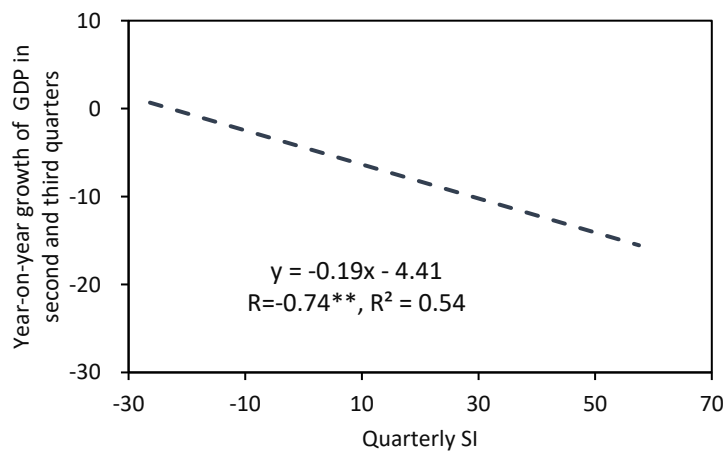


215 **Figure 5.** SI and COVID-19 infection rate in different groups of GNI. (A) The average SI is calculated from the day  
 216 with 100 cumulative COVID-19 cases to Oct. 24, 2020. The horizontal gray line represents the average value of the  
 217 SI, and the vertical gray line represents the average value of the confirmed COVID-19 cases per million population.  
 218 The classification of GNI per capita is based on the method of the World Bank Atlas. (B) Pearson correlation  
 219 coefficient (R) between SI and GNI per capita of 33 countries is -0.57, and there is a significant correlation at the  
 220 0.01 level. (C) Pearson correlation coefficients between COVID-19 infection rate and GNI per capita of 33 countries  
 221 are not significant.  
 222

## 223 Discussion

224 The occasional quietness of the world can be beneficial to our environment and health<sup>33</sup>;  
 225 however, the long-term silence has profound impacts on every aspect of the human system, making  
 226 achievement of SDGs even more urgent<sup>34</sup>. While the impact of the pandemic will vary from country  
 227 to country, it will most likely increase poverty and inequalities on a global scale<sup>35</sup>. A timely  
 228 assessment of the comprehensive impact of COVID-19 is very important. Thus, we constructed the  
 229 silent index (SI), a composite measure of daily human mobility across five place categories and a  
 230 more intuitive and easy-to-understand indicator of lack of mobility at the population level than the  
 231 Google Mobility Index (GMI). Meanwhile, we found a strong linear relationship between quarterly-

232 averaged SI and GDP values (Fig. 6), indicating that, to some extent, SI can reflect the disturbing  
 233 impact of disasters or catastrophic events on the activities related to global or national economy,  
 234 except for reflecting human mobility. Several studies have evaluated the social and economic  
 235 losses<sup>36,37</sup>, and estimated slowdown of GDP for different countries under many scenarios due to the  
 236 impact of COVID-19 pandemic<sup>38,39</sup>. Different from these studies, SI can be used as a real-time  
 237 indicator of slowing economic activities and provide timely data to government and policymakers  
 238 for decision making. For many countries and regions with sufficient Google users, the SI can be  
 239 applied to reflect relative changes in economic activities in real time and at a high temporal  
 240 resolution, which can solve three main problems in traditional economic-statistical indicator data:  
 241 1) lack of the data in certain countries/regions, 2) delay in getting the data, and 3) coarse temporal  
 242 resolution in the data. Thus, the SI be also used as a proxy to quickly and timely monitor the changes  
 243 in human social-economic activities and help public policy decision making at a global scale.



244  
 245 **Figure 6.** A significant linear relationship between SI and GDP growth quarterly. Each dot represents a country. The  
 246 regression equation between SI and GDP growth rate quarterly is  $y = -0.19x - 4.41$ , and there was a significant  
 247 correlation at the 0.01 level. The GDP growth in the second and third quarters can be found in the International  
 248 Monetary Fund (data.imf.org) and the statistical bureau of different countries.

249  
 250 A case study at the urban scale of Italy showed that mobility contraction is stronger in  
 251 municipalities where income per capita is lower<sup>6</sup>, which is consistent with our national-scale result  
 252 In general, the impact of the COVID-19 epidemic on less developed countries and low-income  
 253 populations is more severe, exacerbating the inequalities. Another study has shown that daily  
 254 COVID-19 cases were directly related to the mobility habits 21 days before<sup>40</sup>, which agrees well

255 with our result from 33 countries that the impact of mobility on new COVID-19 cases lagged by at  
256 least 2 weeks. The COVID-19 incidence in some countries showed that the lower the mean income,  
257 the higher the COVID-19 rate<sup>41,42</sup>. However, the analysis based on 33 countries does not show a  
258 significant relationship between national income and COVID-19 incidence (Fig. 5C). At the national  
259 level, the relationship is not yet conclusive.

260 The results of this study indicated that travel restrictions and social policies could take effect  
261 in one week, however, they are difficult to remain effective or be sustainable in the long run. This  
262 might be related to the degree of citizens' cooperation and government interventions<sup>43</sup>. Strict social  
263 distancing policies reduce the severity of the epidemic during the lockdown period, but a full  
264 recovery of the contagion can occur once such measures are relaxed<sup>44</sup>. Thus, a big challenge of the  
265 COVID-19 pandemic is how to balance economic and social activities with epidemic prevention  
266 and control<sup>45,46</sup>. Ideally, we would hope to see a gradual decline in both the silent index and the  
267 number of new cases in the future. To achieve this goal, we need more intelligent social governance,  
268 collaboration on global efforts for prompt and intensive intervention<sup>47</sup>, more effective medical  
269 protection measures, more motivated and educated population practicing evidence-based self-  
270 protection actions, especially in low- and middle-income countries<sup>48</sup>.

271 This study has several limitations. First, we only studied differences at the country level,  
272 without considering the heterogeneity within each country. Second, only Google's mobility data  
273 were applied in this paper, thus some countries such as China and North Korea with few Google  
274 users cannot be evaluated in this study. In the future, the methodological integration of Google,  
275 Apple, Baidu, and other mobile big data can be combined to enlarge the scope and improve the  
276 accuracy of SI. Third, although SI reflects economic development, and maybe some of the place-  
277 specific mobility index captures social activities (e.g., entertainment venue, work place, and park),  
278 we were limited by focusing only on SI to evaluate the impact of COVID. Hence, a comprehensive  
279 consideration of each country's features and combination with other social-economic big data may  
280 further improve the accuracy of the assessment<sup>32</sup>.

281 In summary, compared to the existing literature, the innovation and scientific contribution of  
282 our work are two folds: 1) We estimated the global impact of COVID-19 on human mobility; 2) we  
283 systematically quantified the relationship between mobility, COVID-19 cases, and government

284 response across countries. We observed a drastic impact of the COVID-19 pandemic on human  
285 mobility, which decreased by 12.5% from February to mid-October 2020. Heterogeneity existed in  
286 human mobility reduction across countries and places. Furthermore, bi-directional causality  
287 between SI and COVID-19 new cases was detected with a lagging period of 1-2 weeks, indicating  
288 that the outbreak of COVID-19 pandemic has had a huge impact on mobility, economy and society  
289 of the study countries with lags of one and two weeks. Meanwhile, it showed that the impact of SI  
290 on new COVID-19 cases has a time lag, that is, it cannot take effect quickly in a short period (e.g.,  
291 within a week) but may take at least two weeks to suppress the COVID-19 epidemic. In addition,  
292 the travel restrictions and social policies could take effect in one week, however, they are  
293 challenging to remain effectively in the long run. Finally, SI and GNI per capita have a significant  
294 negative linear relationship; underdeveloped countries are more affected by the COVID-19  
295 epidemic.

## 296 **Methods**

### 297 **Silent index (SI) construction**

298 We take advantage of the advent of mobile location-based services accessed via smartphones, for which daily  
299 data about human mobility are becoming available. In this paper, we collected the Google Mobility Index (GMI)  
300 that show how visits to main place categories change compared to the baseline as a positive or negative percentage  
301 at the country level (<https://www.google.com/covid19/mobility/>). The baseline is the median value, for the  
302 corresponding day of the week, during the 5-week period Jan 3–Feb 6, 2020. Since the penetration of smartphones,  
303 location accuracy of global positioning system data, and the understanding of categorized places vary from region  
304 to region, we selected 33 countries to study the silent index, all of which had high popularity of Google service on  
305 mobile phones and experienced a relatively serious COVID-19 epidemic.

306 In this study, the silent index (SI) was constructed to comprehensively assess the variation of human mobility  
307 at the county level based on Google's mobility big data. The name of this index is inspired by *Silent Spring*, written  
308 by American marine biologist and conservationist Rachel L. Carson, who described the absence of the sound of birds  
309 and insects due to the overutilization of pesticides in the environment<sup>49</sup>. The SI was constructed based on the GMI  
310 in five categorized places (grocery & pharmacy, parks, transit stations, retail & recreation, workplaces) with equal  
311 weights. These places mainly reflect different urban functions including city vitality, economic performance, and  
312 level of epidemic prevention measures (e.g., lockdown and stay-at-home orders), respectively. This SI describes the  
313 relative change of daily human mobility compared with that before the COVID-19 pandemic for a specific region.

314 Further, we calculated a global SI by weighting the SI of each region (i.e., a country in this study) by their populations  
 315 as follows:

$$316 \quad SI_t = -\frac{1}{5} \sum_{i=1}^5 GMI_{it} \quad (1)$$

$$317 \quad Global\_SI_t = \sum_{j=1}^n (SI_{jt} \times W_j) \quad (2)$$

318 In Eq. (1) and (2),  $i$  presents the different categorized places,  $t$  is the date,  $W_j$  is the proportion of the population of  
 319 country  $j$  in the total population of all studied countries,  $n$  is the number of studied countries and regions which is  
 320 126 in this study. Considering the large variation in the SI on weekdays and weekends, and the effect of weather on  
 321 mobility, we use the weekly average to reflect the smooth changes of a long-term series of SI.

### 322 COVID-19 cases data

323 In this study, the total confirmed cases and newly confirmed daily COVID-19 cases at the country level were  
 324 collected from the *WHO Coronavirus Disease (COVID-19) Dashboard* (<https://covid19.who.int/table>). The time  
 325 span of our collected dataset ranges from February 15th to middle October 2020 with a total of 36 weeks. The total  
 326 confirmed number reflects the degree of the impact of COVID-19 in a country, and the newly confirmed cases  
 327 indicate the spread trend of the COVID-19. To compare with SI, we used the number of cases on the last day of the  
 328 week for total confirmed COVID-19 cases and the total number of new cases in one week for newly confirmed cases.  
 329 The baseline day of the COVID-19 pandemic is considered when cumulatively 100 confirmed COVID-19 cases  
 330 were reported. The country-level population used in the calculation of confirmed COVID-19 cases per million  
 331 population comes from the World Development Index database 2020  
 332 (<https://databank.worldbank.org/reports.aspx?source=world-development-indicators>).

### 333 Policy stringency index (PI)

334 It was revealed that the government response measures play a critical role in stemming the infection of COVID-  
 335 19<sup>50</sup>. Government interventions to the COVID-19 spread was measured by policy stringency index (PI) designed by  
 336 the University of Oxford combining a series of indices to aggregate various measures of government responses to  
 337 COVID-19 ([www.bsg.ox.ac.uk/covidtracker](http://www.bsg.ox.ac.uk/covidtracker))<sup>51</sup>. PI was created into a composite score between 0 and 100, which  
 338 included government restrictions and closing of school, workplace, public transport, restrictions on internal and  
 339 international movement, and other economic, containment, and health measures, etc. (see Table S2). PI was  
 340 calculated as follows:

$$341 \quad I_{kt} = 100 \frac{v_{kt} - 0.5(F_k - f_{kt})}{N_k} \quad (3)$$

$$342 \quad PI = \frac{1}{n} \sum_{k=1}^n I_k \quad (4)$$

343 In Eq. (3) and (4),  $I$  means each sub-index score for any given indicator ( $k$ ) on any given day ( $t$ );  $N_k$  is the maximum  
 344 value of the indicator, whether that indicator has a flag ( $F_k=1$  if the indicator has a flag variable, or 0 if the indicator  
 345 does not have a flag variable), the recorded policy value on the ordinal scale ( $v_{kt}$ ), the recorded binary flag for that  
 346 indicator, if that indicator has a flag ( $f_{kt}$ ).

### 347 Hierarchical clustering

348 We obtained a clustered heatmap using the hierarchical clustering method (Fig. S1) <sup>52</sup>. The order of the rows is  
 349 determined by performing hierarchical cluster analyses of the rows, which tend to position similar rows together on  
 350 the plot. In this study, the hierarchical clustering was calculated of SI variation from the baseline day to middle  
 351 October 2020 with the dendrogram in the heatmap of the selected countries. The analysis was performed through  
 352 the R software with essential package *gplots*<sup>53</sup>.

### 353 Panel vector autoregression (PVAR)

#### 354 PVAR modeling

355 One of the main aims of this study was to investigate the potential bi-directional causal relationship between SI  
 356 and the growth rate of new COVID-19 cases. The increase of SI may slow down the spread of COVID-19, while the  
 357 increase in newly confirmed cases may cause an increase in SI. The panel vector autoregression (PVAR) model has  
 358 been widely applied to examine causal relationships of financial conditions and investment<sup>54</sup>, the impact of  
 359 renewable energy and financial development on carbon dioxide emissions and economic growth<sup>55</sup>, and the dynamics  
 360 of mental well-being and other social factors<sup>56</sup>. The PVAR considers all variables and lag periods to reflect the  
 361 interactive relationship of each variable; all variables are typically treated as endogenous in the PVAR<sup>57</sup>, which is  
 362 valid for causality analysis with time-series data. In this study, general methods of the moment were applied in the  
 363 PVAR to detect the dynamic relationship between SI and the growth rate of new COVID-19 cases.

364 The PVAR models can be constructed as the following. Among them, models (5) and (6) were constructed to  
 365 reveal the direct effect of SI on suppressing the growth rate of new COVID-19 cases, and models (7) and (8) were  
 366 constructed to probe the relationship between SI and PI.

$$367 \quad D.addcase_{j,t} = w_0 + \sum_{l=1}^n \alpha_l D.addcase_{j,t-l} + \sum_{l=1}^n \beta_l SI_{j,t-l} + f_j + \varphi_t + u_{jt} \quad (5)$$

$$368 \quad SI_{j,t} = \varepsilon_0 + \sum_{l=1}^n \gamma_l SI_{j,t-l} + \sum_{l=1}^n \theta_l D.addcase_{j,t-l} + f_j + \varphi_t + u_{jt} \quad (6)$$

$$369 \quad PI_{j,t} = w_0 + \sum_{l=1}^n \alpha_l PI_{j,t-l} + \sum_{l=1}^n \beta_l SI_{j,t-l} + f_j + \varphi_t + u_{jt} \quad (7)$$

$$370 \quad SI_{j,t} = \varepsilon_0 + \sum_{l=1}^n \gamma_l SI_{j,t-l} + \sum_{l=1}^n \theta_l PI_{j,t-l} + f_j + \varphi_t + u_{jt} \quad (8)$$

371 In the above equations,  $D.addcase_{j,t-1}$ ,  $SI_{j,t-1}$ , and  $PI_{j,t-1}$  indicated the explanatory variables based on the  $l$ -order lag  
 372 period of the growth rate of new COVID-19 cases per million people per week (i.e., the first-order difference of

373 newly confirmed cases), the silent index, and the policy stringency index (PI). Meanwhile,  $\alpha_i$ ,  $\gamma_i$ ,  $\beta_i$  and  $\theta_i$  were the  
374 estimated coefficients of each lagged explanatory variable.  $f_j$  represented the individual fixed effect in PVAR  
375 modeling to consider the heterogeneity across the country.  $\varphi_t$  represented the time fixed effect.  $u_{jt}$  represented the  
376 random disturbance term, and  $w_0$  and  $\varepsilon_0$  were the intercepts. The subscripts  $i$ ,  $j$ , and  $t$  represented the number of lag  
377 periods, different countries, and dates, respectively. Combining the three criteria of MBIC, MAIC, and MQIC, we  
378 found that the optimal lag orders of the two sets of PVAR models are both lagging by 2 periods (see Table S4-S5).

#### 379 *Unit root test*

380 Additionally, before the PVAR, the unit root test was conducted to avoid false regression<sup>58</sup>. In this study, two  
381 widely used panel unit test methods were adopted, namely the LLC test for common root tests and the IPS test and  
382 the Fisher-ADF test for heterogeneous unit root tests. The test results were shown in Table S3. All three variables  
383 passed the unit root test, indicating the stationarity of these panel data.

#### 384 **Impulse response function (IRF)**

385 The impulse response functions (IRF) were derived from the estimated quadrivariate VAR models by using the  
386 Cholesky decomposition method<sup>59</sup>. This method can describe the evolution of a model's variables in reaction to a  
387 shock in one or more variables, and this feature allows us to trace the transmission of a single shock within an  
388 otherwise noisy system of equations. Hence, in this study, the IRF depicts the changing trend of the impact of the  
389 change of SI on the growth rate of new COVID-19 cases, the changing trend of the impact of the growth rate of new  
390 COVID-19 cases on SI, and the dynamic relationship between SI and policy stringency index.

#### 391 **Data availability**

392 All input data used in these analyses were derived from published sources cited in the Methods.  
393 Any other datasets generated in the current study are available from the corresponding author upon  
394 request.

#### 395 **References**

- 396 1. Economic and Social Council, United Nations. *Progress towards the Sustainable Development*  
397 *Goals*. (2020).
- 398 2. Transition from pandemic. *Nature Sustainability* **3**, 345–345 (2020).
- 399 3. Nguyen, M. H. *et al.* Changes in digital communication during the COVID-19 global pandemic:

- 400 Implications for digital inequality and future research. *Social Media+ Society* **6**, (2020).
- 401 4. Hsiang, S. *et al.* The effect of large-scale anti-contagion policies on the COVID-19 pandemic.  
402 *Nature* **584**, 262–267 (2020).
- 403 5. Lai, S. *et al.* Effect of non-pharmaceutical interventions to contain COVID-19 in China. *Nature*  
404 **585**, 410–413 (2020).
- 405 6. Bonaccorsi, G. *et al.* Economic and social consequences of human mobility restrictions under  
406 COVID-19. *Proceedings of the National Academy of Sciences* **117**, 15530–15535 (2020).
- 407 7. Susskind, D. & Vines, D. The economics of the COVID-19 pandemic: an assessment. *Oxford*  
408 *Review of Economic Policy* **36**, S1–S13 (2020).
- 409 8. Gössling, S., Scott, D. & Hall, C. M. Pandemics, tourism and global change: a rapid assessment  
410 of COVID-19. *Journal of Sustainable Tourism* 1–20 (2020).
- 411 9. Guerriero, C., Haines, A. & Pagano, M. Health and sustainability in post-pandemic economic  
412 policies. *Nature Sustainability* **3**, 494–496 (2020).
- 413 10. Alon, T. M., Doepke, M., Olmstead-Rumsey, J. & Tertilt, M. *The impact of COVID-19 on gender*  
414 *equality*. (2020).
- 415 11. Van Lancker, W. & Parolin, Z. COVID-19, school closures, and child poverty: a social crisis in the  
416 making. *The Lancet Public Health* **5**, e243–e244 (2020).
- 417 12. Sumner, A., Hoy, C. & Ortiz-Juarez, E. Estimates of the Impact of COVID-19 on Global Poverty.  
418 *UNU-WIDER, April* 800–9 (2020).
- 419 13. Brownstein, J. S., Freifeld, C. C. & Madoff, L. C. Digital disease detection—harnessing the Web  
420 for public health surveillance. *The New England journal of medicine* **360**, 2153 (2009).
- 421 14. Szocska, M. *et al.* Countrywide population movement monitoring using mobile devices

- 422 generated (big) data during the COVID-19 crisis. *Scientific Reports* **11**, 5943 (2021).
- 423 15. Huang, X. *et al.* The characteristics of multi-source mobility datasets and how they reveal the  
424 luxury nature of social distancing in the US during the COVID-19 pandemic. *medRxiv* (2020).
- 425 16. Kang, Y. *et al.* Multiscale dynamic human mobility flow dataset in the US during the COVID-19  
426 epidemic. *Scientific data* **7**, 1–13 (2020).
- 427 17. Warren, M. S. & Skillman, S. W. Mobility changes in response to COVID-19. *arXiv preprint*  
428 *arXiv:2003.14228* (2020).
- 429 18. Chinazzi, M. *et al.* The effect of travel restrictions on the spread of the 2019 novel coronavirus  
430 (COVID-19) outbreak. *Science* **368**, 395 (2020).
- 431 19. Kraemer, M. U. G. *et al.* The effect of human mobility and control measures on the COVID-19  
432 epidemic in China. *Science* **368**, 493 (2020).
- 433 20. Tian, H. *et al.* An investigation of transmission control measures during the first 50 days of the  
434 COVID-19 epidemic in China. *Science* **368**, 638 (2020).
- 435 21. Schlosser, F. *et al.* COVID-19 lockdown induces disease-mitigating structural changes in  
436 mobility networks. *Proceedings of the National Academy of Sciences* **117**, 32883–32890 (2020).
- 437 22. Oh, J. *et al.* How well does societal mobility restriction help control the COVID-19 pandemic?  
438 Evidence from real-time evaluation. (2020).
- 439 23. Lasry, A. *et al.* Timing of community mitigation and changes in reported COVID-19 and  
440 community mobility—four US metropolitan areas, February 26–April 1, 2020. *Morbidity and*  
441 *Mortality Weekly Report* **69**, 451–457 (2020).
- 442 24. Gao, S. *et al.* Association of mobile phone location data indications of travel and stay-at-home  
443 mandates with covid-19 infection rates in the us. *JAMA network open* **3**, e2020485–e2020485

- 444 (2020).
- 445 25. Yilmazkuday, H. Stay-at-Home Works to Fight Against COVID-19: International Evidence from  
446 Google Mobility Data. *Available at SSRN 3571708* (2020).
- 447 26. McKenzie, G. & Adams, B. A country comparison of place-based activity response to COVID-  
448 19 policies. *Applied Geography* **125**, 102363 (2020).
- 449 27. Carteni, A., Di Francesco, L. & Martino, M. How mobility habits influenced the spread of the  
450 COVID-19 pandemic: Results from the Italian case study. *Science of the Total Environment* **741**,  
451 140489 (2020).
- 452 28. Flaxman, S. *et al.* Estimating the effects of non-pharmaceutical interventions on COVID-19 in  
453 Europe. *Nature* **584**, 257–261 (2020).
- 454 29. Frias-Martinez, V., Virseda, J. & Frias-Martinez, E. Socio-economic levels and human mobility.  
455 in *Qual meets quant workshop-QMQ* 1–6 (2010).
- 456 30. Soto, V., Frias-Martinez, V., Virseda, J. & Frias-Martinez, E. Prediction of socioeconomic levels  
457 using cell phone records. in 377–388 (Springer, 2011).
- 458 31. Pappalardo, L., Pedreschi, D., Smoreda, Z. & Giannotti, F. Using big data to study the link  
459 between human mobility and socio-economic development. in *2015 IEEE International  
460 Conference on Big Data (Big Data)* 871–878 (IEEE, 2015).
- 461 32. Xu, Y., Belyi, A., Bojic, I. & Ratti, C. Human mobility and socioeconomic status: Analysis of  
462 Singapore and Boston. *Computers, Environment and Urban Systems* **72**, 51–67 (2018).
- 463 33. Chen, K., Wang, M., Huang, C., Kinney, P. L. & Anastas, P. T. Air pollution reduction and mortality  
464 benefit during the COVID-19 outbreak in China. *The Lancet Planetary Health* **4**, e210–e212  
465 (2020).

- 466 34. Mofijur, M. *et al.* Impact of COVID-19 on the social, economic, environmental and energy  
467 domains: Lessons learnt from a global pandemic. *Sustainable production and consumption*  
468 (2020).
- 469 35. United Nations. *A UN framework for the immediate socio-economic response to COVID-19*.  
470 (2020).
- 471 36. Lenzen, M. *et al.* Global socio-economic losses and environmental gains from the Coronavirus  
472 pandemic. *PLoS One* **15**, e0235654 (2020).
- 473 37. Liu, H., Fang, C. & Gao, Q. Evaluating the Real-Time Impact of COVID-19 on Cities: China as a  
474 Case Study. *Complexity* **2020**, (2020).
- 475 38. Fernandes, N. Economic effects of coronavirus outbreak (COVID-19) on the world economy.  
476 *Available at SSRN 3557504* (2020).
- 477 39. World Bank. *Global Economic Prospects, June 2020*. (The World Bank, 2020).
- 478 40. Carteni, A., Di Francesco, L. & Martino, M. How mobility habits influenced the spread of the  
479 COVID-19 pandemic: Results from the Italian case study. *Science of the Total Environment* **741**,  
480 140489 (2020).
- 481 41. Baena-Díez, J. M., Barroso, M., Cordeiro-Coelho, S. I., Díaz, J. L. & Grau, M. Impact of COVID-  
482 19 outbreak by income: hitting hardest the most deprived. *Journal of Public Health* **42**, 698–  
483 703 (2020).
- 484 42. Huang, X. *et al.* Time-series clustering for home dwell time during COVID-19: what can we  
485 learn from it? *ISPRS International Journal of Geo-Information* **9**, 675 (2020).
- 486 43. Haug, N. *et al.* Ranking the effectiveness of worldwide COVID-19 government interventions.  
487 *Nature human behaviour* 1–10 (2020).

- 488 44. Scala, A. *et al.* Time, space and social interactions: exit mechanisms for the Covid-19 epidemics.  
489 *Scientific Reports* **10**, 13764 (2020).
- 490 45. Cornwall, W. Can you put a price on COVID-19 options? Experts weigh lives versus economics.  
491 *Science* **10**, (2020).
- 492 46. Askitas, N., Tatsiramos, K. & Verheyden, B. Estimating worldwide effects of non-  
493 pharmaceutical interventions on COVID-19 incidence and population mobility patterns using  
494 a multiple-event study. *Scientific Reports* **11**, 1972 (2021).
- 495 47. Li, R. *et al.* Global COVID-19 pandemic demands joint interventions for the suppression of  
496 future waves. *Proceedings of the National Academy of Sciences* **117**, 26151–26157 (2020).
- 497 48. Walker, P. G. *et al.* The impact of COVID-19 and strategies for mitigation and suppression in  
498 low-and middle-income countries. *Science* (2020).
- 499 49. Carson, R. *Silent spring*. (Houghton Mifflin Harcourt, 1962).
- 500 50. Gates, B. Responding to Covid-19—a once-in-a-century pandemic? *New England Journal of*  
501 *Medicine* **382**, 1677–1679 (2020).
- 502 51. Hale, T., Petherick, A., Phillips, T. & Webster, S. Variation in government responses to COVID-  
503 19. *Blavatnik School of Government Working Paper* **31**, (2020).
- 504 52. Murtagh, F. & Contreras, P. Algorithms for hierarchical clustering: an overview, II. *Wiley*  
505 *Interdisciplinary Reviews: Data Mining and Knowledge Discovery* **7**, e1219 (2017).
- 506 53. Warnes, M. G. R., Bolker, B., Bonebakker, L., Gentleman, R. & Huber, W. Package ‘gplots’.  
507 *Various R Programming Tools for Plotting Data* (2016).
- 508 54. Love, I. & Zicchino, L. Financial development and dynamic investment behavior: Evidence from  
509 panel VAR. *The Quarterly Review of Economics and Finance* **46**, 190–210 (2006).

- 510 55. Charfeddine, L. & Kahia, M. Impact of renewable energy consumption and financial  
511 development on CO2 emissions and economic growth in the MENA region: A panel vector  
512 autoregressive (PVAR) analysis. *Renewable Energy* **139**, 198–213 (2019).
- 513 56. Binder, M. & Coad, A. An examination of the dynamics of well-being and life events using  
514 vector autoregressions. *Journal of Economic Behavior & Organization* **76**, 352–371 (2010).
- 515 57. Holtz-Eakin, D., Newey, W. & Rosen, H. S. Estimating vector autoregressions with panel data.  
516 *Econometrica: Journal of the Econometric Society* 1371–1395 (1988).
- 517 58. Perron, P. The great crash, the oil price shock, and the unit root hypothesis. *Econometrica:*  
518 *journal of the Econometric Society* 1361–1401 (1989).
- 519 59. Enders, W. *Applied econometric time series*. (John Wiley & Sons, 2008).
- 520

521 **Author contributions statement**

522 H. L. designed and performed the research, led the collaborative work, and preparation of the  
523 figures. S. W. contributed to data collection, data analysis, and preparation of the manuscript. Y. T.  
524 and Y. F. contributed to data analysis, and preparation of the manuscript. J. W., Z. W. and C. F.  
525 contributed to review and editing.

526

527 **Additional Information**

528 The authors declare no competing interests.

529

530 **Acknowledgements**

531 Funding for this work was provided by the National Natural Science Foundation of China (no.  
532 41801164) and China Association for Science and Technology (20200608CG072501).

533

534

# Figures

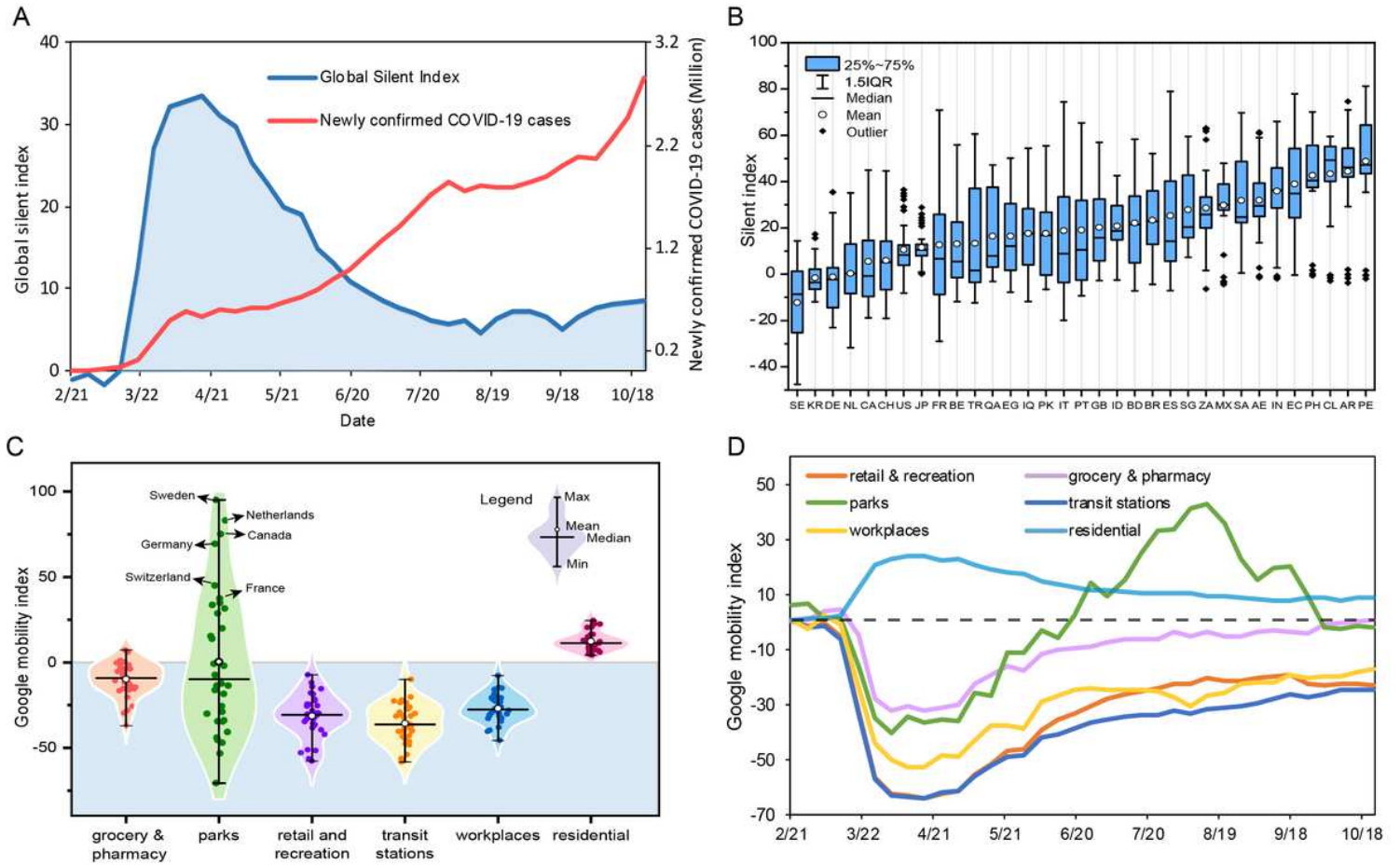


**Figure 1**

Variation of the silent world globally, nationally and by place. (A) Temporal variation of global SI and the number of newly confirmed COVID-19 cases from 126 countries from the baseline day to middle October 2020. (B) Box-plot of SI since the 100 confirmed COVID-19 cases reported in 33 selected countries. (C) Violin-plot of Google mobility index (see Methods) by six place categories in 33 countries. (D) Temporal variation of mobility in six places in 33 countries.

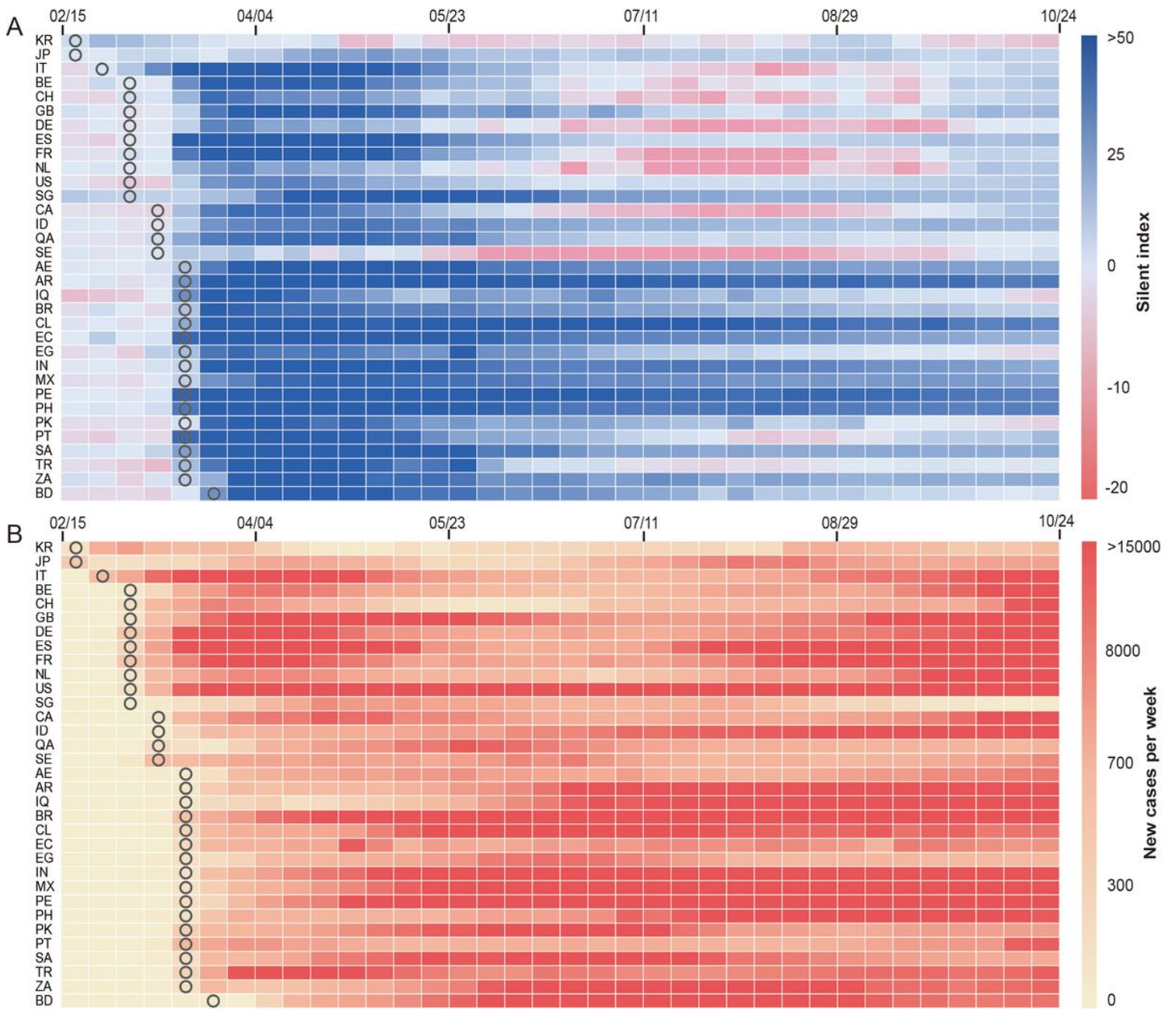


**Figure 2**

Temporal variations of SI and new COVID-19 cases. The changing of SI (A) and newly confirmed weekly cases of COVID-19 (B) in 33 selected countries from the baseline day to late October 2020 were visualized with heatmap. The symbol “○” indicated the week when the cumulative number of COVID-19 cases reached 100. The 33 countries’ full names can be seen in Table S1.

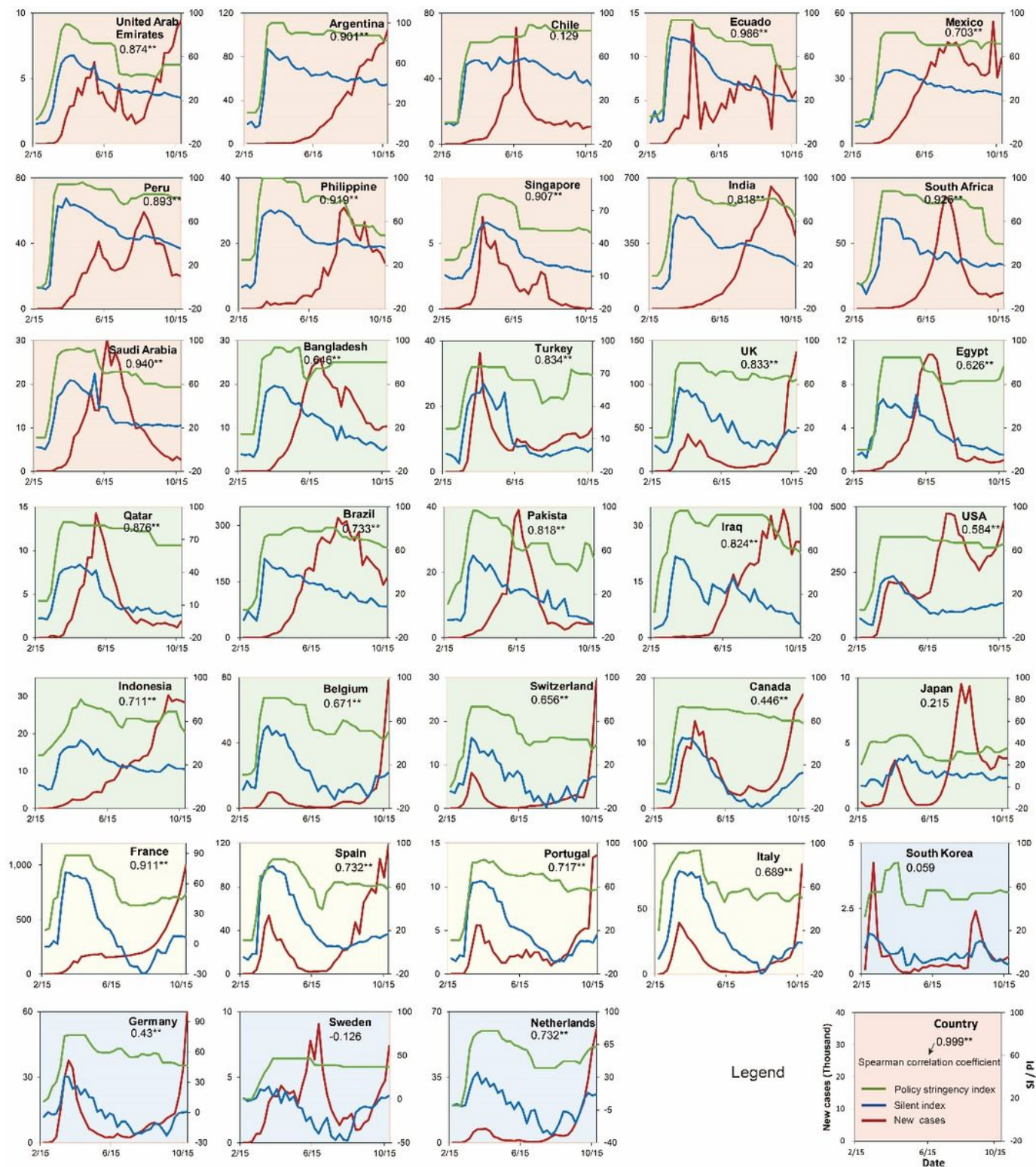


**Figure 3**

Temporal variation of SI, the new COVID-19 cases, and policy stringency index by countries. Four groups across the countries are clustered with different colors by dendrogram in the heatmap of SI (see Fig. S1). Spearman correlations between SI and PI are labeled for each country, and \*\* means a significant correlation at the 0.01 level.

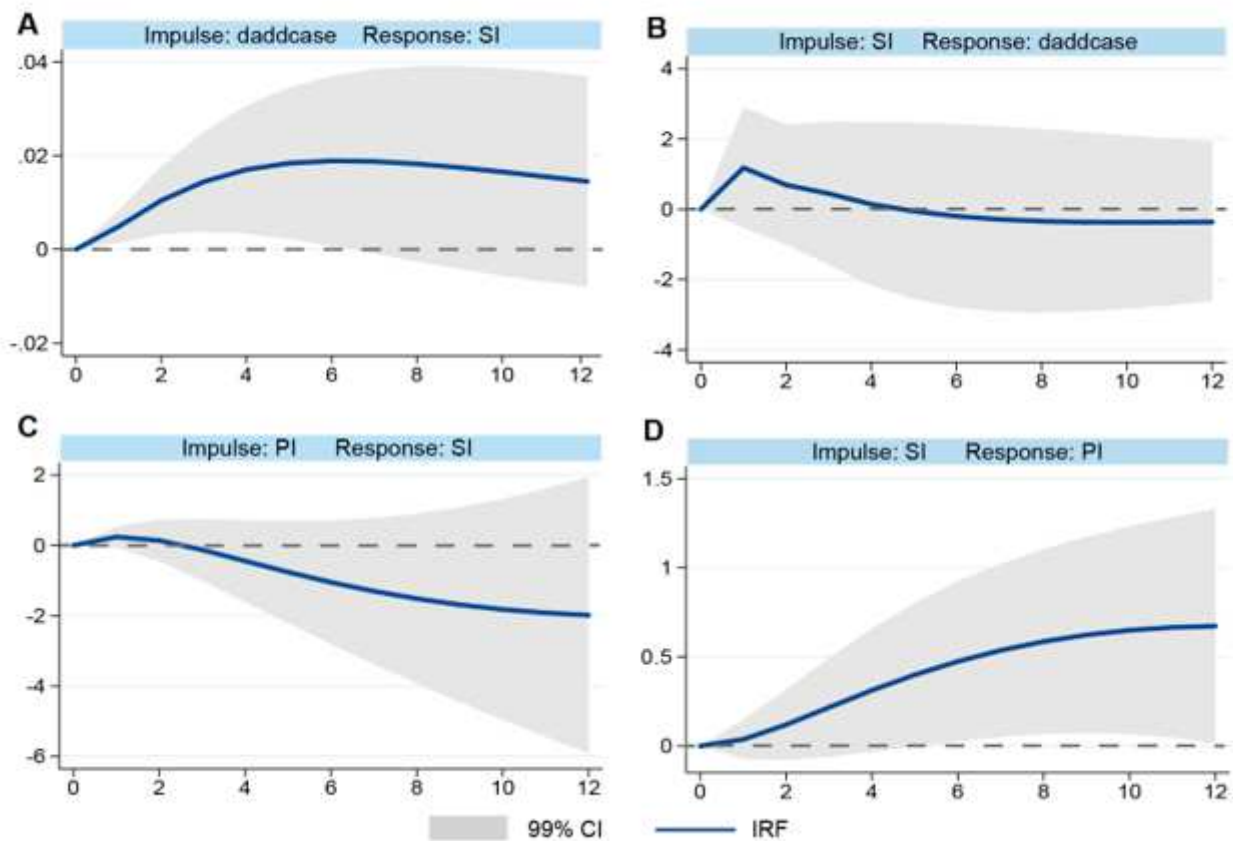


**Figure 4**

Results of impulse response function (IRF) analysis. Impulse response results were obtained by running 500 iterations of the Monte Carlo Simulation; the upper and lower curves represent the 99% CI. The horizontal axis indicates the step numbers of the twelve-period impulse response function.

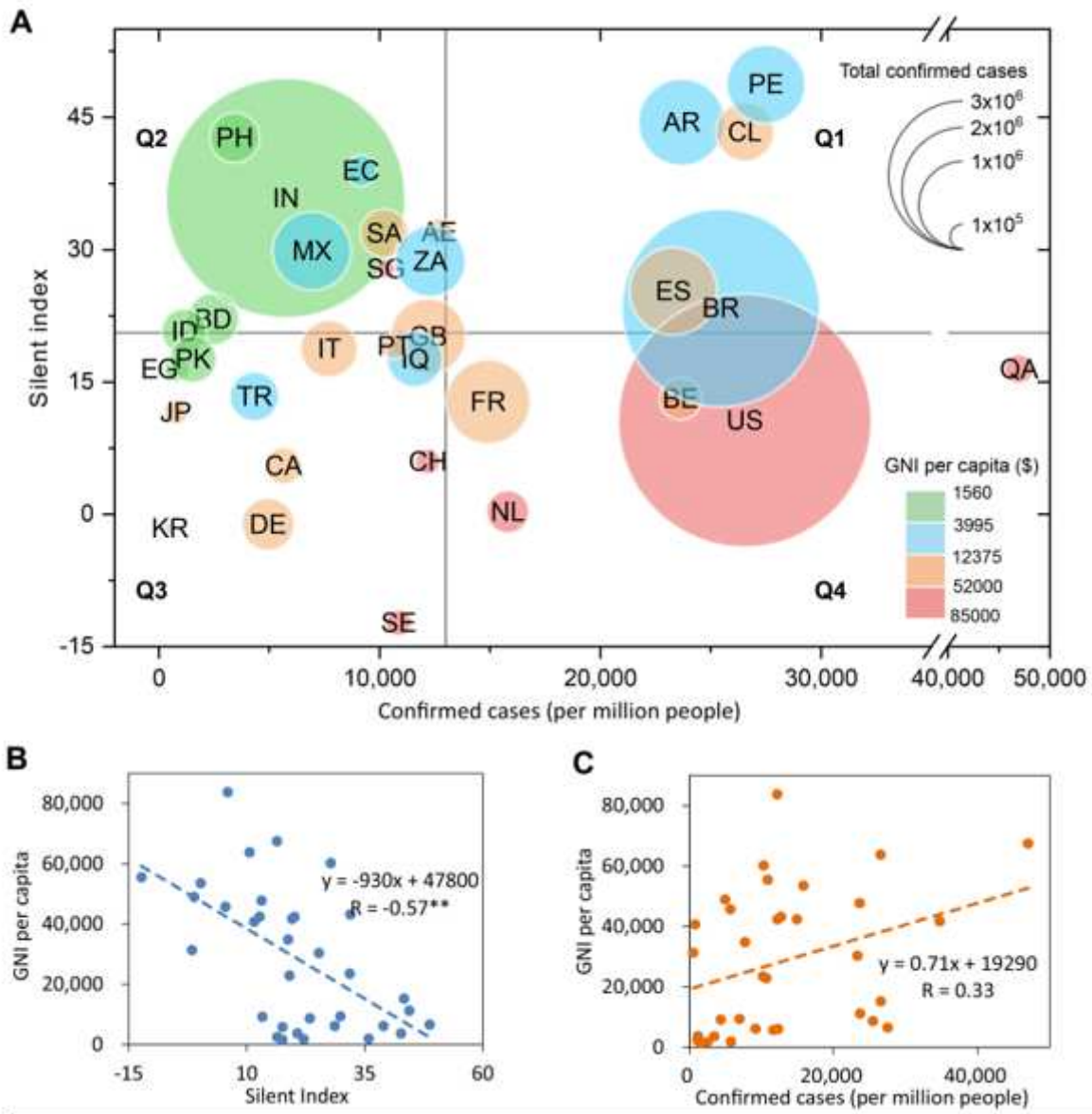


**Figure 5**

SI and COVID-19 infection rate in different groups of GNI. (A) The average SI is calculated from the day with 100 cumulative COVID-19 cases to Oct. 24, 2020. The horizontal gray line represents the average value of the SI, and the vertical gray line represents the average value of the confirmed COVID-19 cases per million population. The classification of GNI per capita is based on the method of the World Bank Atlas. (B) Pearson correlation coefficient ( $R$ ) between SI and GNI per capita of 33 countries is -0.57, and there is a significant correlation at the 0.01 level. (C) Pearson correlation coefficients between COVID-19 infection rate and GNI per capita of 33 countries are not significant.

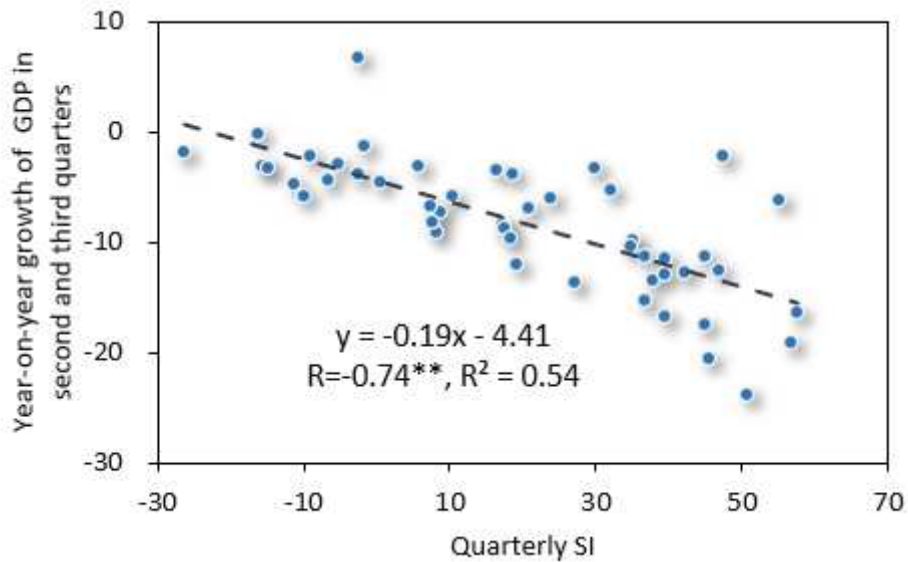


**Figure 6**

A significant linear relationship between SI and GDP growth quarterly. Each dot represents a country. The regression equation between SI and GDP growth rate quarterly is  $y = -0.19x - 4.41$ , and there was a significant correlation at the 0.01 level. The GDP growth in the second and third quarters can be found in the International Monetary Fund (data.imf.org) and the statistical bureau of different countries.

## Supplementary Files

This is a list of supplementary files associated with this preprint. Click to download.

- [Supplementarymaterial0331.docx](#)